Investigation of the adsorption of a mixture of two anionic surfactants, AOT and SDBS, on silica at ambient temperature

Julie Wolanin, Loïc Barré, Christine Dalmazzone, Daniela Bauer

Title.

Investigation of the adsorption of a mixture of two anionic surfactants, AOT and SDBS, on silica at ambient temperature

Author names and affiliations.

Julie WOLANIN[a], Loïc BARRÉ[a], Christine DALMAZZONE[a] and Daniela BAUER[a]

[a] IFP Energies nouvelles, 1 et 4 avenue du Bois-Préau, 92852, Rueil Malmaison, France

Corresponding author. Christine DALMAZZONE (email: christine.dalmazzone@ifp.fr ; postal address: IFP Energies nouvelles, 1 et 4 avenue du Bois-Préau, 92852, Rueil Malmaison, France)

Keywords.

Surfactant mixtures; vesicle; adsorption; QCM-D; neutron reflectivity.

Abstract

Chemical flooding, one of the Enhanced Oil Recovery (EOR) techniques used to increase oil production, consists in the injection in the well of an aqueous formulation containing various chemical additives such as surfactants. However, its performance can be significantly altered by the loss of surfactants in reservoir rocks. More precisely, surfactant loss due to adsorption on the reservoir rock may have a non-negligible impact on the efficiency of the injected formulation. In this article, we considered the adsorption of a mixture of two anionic surfactants having an important industrial relevance for EOR applications. Adsorption was studied on silica, representative of reservoir rocks such as sandstone, by combining Quartz Crystal Microbalance with Dissipation monitoring (QCM-D) and neutron reflectivity experiments. A preliminary characterization of the surfactant mixture solution demonstrated the formation of unilamellar vesicles in the bulk. Whereas an adsorbed layer was measured with the single AOT vesicles, but not with the SDBS micelles, we observed that mixing both anionic surfactants change the adsorption phenomenon. Indeed, non-negligible adsorption was measured for the mixture even at concentrations where only slight adsorption had been observed with the individual surfactants. This suggests that the structure of the aggregates formed in the bulk has a non-negligible impact on the adsorption. We note that the addition of salt tends to enhance the adsorption by screening the repulsive interactions between both negatively charged surfactants and silica at neutral pH. The present work provides new insights into the description of the adsorption of a mixture of surfactants of same nature in unfavorable conditions.

Graphical abstract.

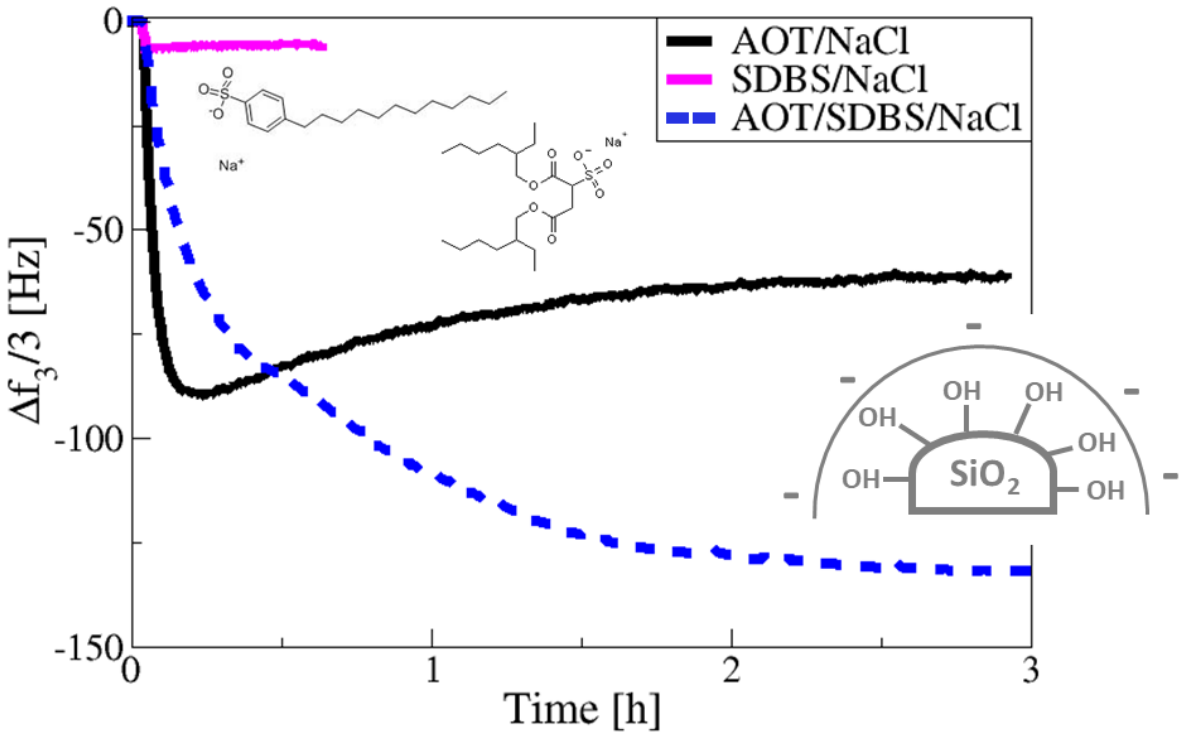

1. Introduction

Surfactants are used in many industrial processes (detergency, cosmetics, pharmaceutics, food, oil recovery …). Most of the commercial surfactant systems are mixtures of surfactants that are much more effective than systems containing a single surfactant. In Enhanced Oil Recovery processes (EOR), a chemical formulation containing a surfactant mixture is injected into the well in order to mobilize the oil trapped in the rock reservoir by lowering the interfacial tension between oil and water. The efficiency of the injected formulation can be significantly affected by the non-negligible loss of surfactants due to adsorption on the rock surface. In this way, the overall process may become uneconomical. Mixtures of anionic surfactants are generally used in EOR processes because of their interesting economical and physico-chemical properties as their lower cost, high capacity of interfacial tension reduction, low adsorption on sandstone (globally negatively charged) and thermal stability (sulfonate surfactants are stable above 200°C).

Due to their improved physico-chemical properties, chemical formulations containing a mixture of surfactants can be used under a wider range of experimental conditions than those containing a single surfactant (high pressure and temperature, wide range of salinity concentrations…). However, the adsorption behavior can be considerably impacted by the use of a mixture due to the interactions between the two surfactants themselves.

The adsorption of single surfactants at the solid/liquid interface has been widely studied over the past decades [1–10]. Also, many studies involving the adsorption of surfactant mixtures of different types (anionic–cationic [11,12], anionic–nonionic [12,13], cationic–nonionic [12], cationic–zwitterionic [12]) can be found in the literature. However, only few studies exist dealing with the adsorption of a mixture of surfactants of the same type such as two anionic surfactants. Indeed, in this article, we investigated a mixture of two anionic surfactants relevant in chemical EOR processes where a mixture of anionic surfactants is injected into the well.

In the case of anionic/non-ionic surfactant mixtures, most of the studies have demonstrated synergistic adsorption [12,14]. The increase in adsorption is attributed to the decrease of the electrostatic repulsions between the negatively charged heads of the anionic surfactant resulting from the insertion of the nonionic surfactant between them. The adsorption is also favoured by the reduction of the water molecules in the hydrophobe-rich structure promoting the inter-chains interactions. Thus, both relative and absolute lengths of hydrophobic chains have a significant impact on the adsorption enhancement. However, Zhang et al. [12] have shown that both an antagonistic and synergistic effects could be measured, according to the experimental conditions. Muherei et al. [14] have demonstrated the lowering of the adsorption of Triton X-100 (non-ionic) on clay after the addition of sodium dodecyl sulfate (anionic). On the other side, anionic–cationic surfactant mixtures have been the objective of only a few studies due to their tendency to precipitate. However, Huang et al. [11] have demonstrated that the adsorption of anionic surfactants on silica can be enhanced by the addition of cationic surfactant with the formation of ion-pairs. Finally, only few articles exist on the adsorption of anionic surfactant mixtures [15–18] and most of these studies focused on anionic fluorocarbon-anionic hydrocarbon surfactants mixtures [19–21].

In the present article, we investigated the adsorption of a mixture of two anionic surfactants (AOT and SDBS, α_{AOT} =0.8 with α_{AOT} being the AOT molar fraction) in a brine solution on silica. The latter has been chosen to mimic the rock reservoirs. Because oil

reservoirs are usually in saline conditions, we studied adsorption in a brine composed of 15 g/L of sodium chloride. In the following, we provide, in a first step, the results regarding the characterization of bulk surfactant aggregates. We then present the adsorption experiments considering the individual surfactants as well as their mixtures, followed by a discussion.

2. Materials and Methods

2.1. Materials

AOT (sodium bis(2-ethyl-1-hexyl)sulfosuccinate, $C_{20}H_{37}NaO_7S$, BioXtra, purity ≥ 99%) and SDBS (sodium dodecylbenzenesulfonate, $C_{12}H_{25}C_6H_4SO_3Na$, technical grade, purity < 90%) were purchased from Sigma-Aldrich and used without further purification. Their chemical structures are presented in Figure 1. The certificates of analysis provided by the supplier give the identification of AOT cationic impurities (potassium < 0.01%, calcium, lead and aluminum < 0.001%, magnesium, iron, zinc, copper and phosphorus < 0.0005%, and insoluble matter < 0.1%) and SDBS impurities (positional isomers, isomers of various chain lengths, branched isomers or non-sulfonated alkyl chains). HPLC characterization of both surfactants gives a single peak for AOT and shows peak splitting for SDBS that can be attributed to the presence of isomers.

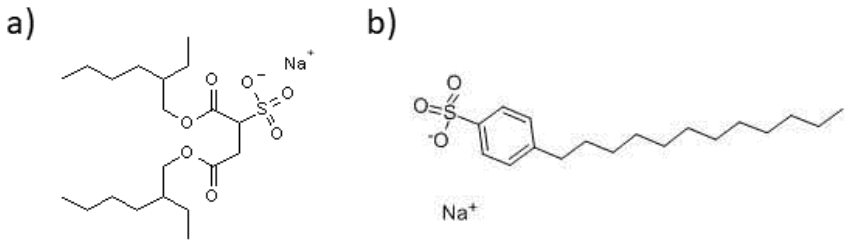

Figure 1 : Chemical structure of a) AOT b) SDBS

Water was obtained from a Millipore system and D_2O was purchased from Eurisotop (99.96% D). NaCl was purchased from Fischer Chemical (purity>99%). The main cationic impurities were calcium (0.005%), iodide (0.002%) and magnesium (0.005%).

We used an AOT/SDBS solution with an AOT molar fraction, α_{AOT}, fixed to 0.8. Surfactants were diluted in brine composed of 15 g/L NaCl. The measured pH of the surfactant solutions is 6, thus the silica surface is supposed to be slightly negatively charged due to the high electrolyte concentration causing a considerable decrease of the Debye length (estimated to ~ 0.6 nm in comparison to ~ 100 nm in the case of no salt addition) [22]. Singh et al. [23] have shown that the AOT/SDS (sodium dodecyl sulfate, an anionic surfactant) mixture exhibits ideality when the AOT molar fraction, α_{AOT}, is higher than 0.7. An ideal behavior assumes that the interactions between the surfactants in the mixture are similar to those between the identical surfactants themselves. Based on the results presented by Singh et al. [23] we supposed that the AOT/SDS behavior is similar to that of AOT/SDBS. Thus, we fixed α_{AOT} to 0.8 assuming that the selected mixture exhibits ideality. This assumption is supported by the fact that the two investigated anionic surfactants have the same sulfonate hydrophilic group.

It has already been reported in the literature [10,24] that impurities can bind to the surface and have an impact on the adsorption phenomenon. Surfactants and NaCl were not purified

for this study as in commercially relevant systems, unpurified chemicals are generally used. Impurities are often multiple cations and organic molecules, which are in competition with the chemicals for the adsorption. The relevance of impurities coming from surfactants or NaCl can be estimated from the surface tension plots as proposed by Li et al. [25]. In the surface tension plots obtained with the Wilhelmy plate method (Figure 2), we observe characteristic features of impure surfactants solutions (a shallow slope and a surface tension tending toward a lower value than the expected 72 mN/m measured for water with no surfactants). These characteristics are generated by the presence of divalent cationic impurities co-adsorbed in the surfactant layer at the air/water interface. Even if in the method used (QCM-D), where only a very small amount of surfactant is adsorbed, the effects of impurities are amplified compared to a method of adsorption on large surface area particulates, the possible influence of the impurities can be neglected because of the very low surfactant concentrations investigated.

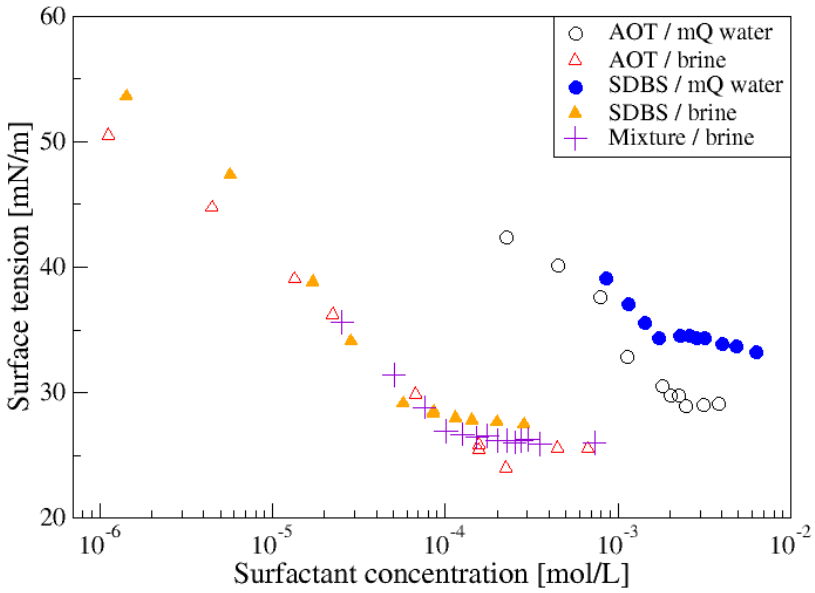

Figure 2 : Surface tension versus molar surfactant concentration plots

The Critical Aggregation Concentration values (CAC, defined as the concentration above which surfactant aggregates start to form in solution) obtained for the different systems (AOT, SDBS and AOT/SDBS mixture) are presented in Table 1. Above the CAC, the AOT/brine system (packing parameter comprised between 0.5 and 1) mainly forms small unilamellar vesicles (14 nm diameter) in solution; details on the characterization of this solution can be found in the literature [26]. The SDBS/brine system (packing parameter < 1/3) was supposed to form spherical or cylindrical micelles [27] as spontaneous formation of vesicles in solution has only been reported and measured at higher surfactant (3.5 g/L) and brine (NaCl 21 g/L) concentrations [28]. Thus, we called CVC_{AOT} and CMC_{SDBS}, the Critical Vesicular Concentration of AOT and the Critical Micellar Concentration of SDBS, respectively, in the same brine solution.

Table 1 : Measurements of the Critical Aggregation Concentration values (CACs) of the investigated systems in brine (15 g/L NaCl) with the Wilhelmy plate method

	AOT in brine	**SDBS in brine**	**AOT/SDBS (α_{AOT}=0.8) in brine**	
			AOT	SDBS
CAC [g/L]	0.09	0.02	0.045	0.009

CAC [mol/L]	2.02E-04	5.74E-05	1.01E-04	2.58E-05

2.2. Methods

2.2.1. Cryo-Transmission Electron Microscopy (Cryo-TEM)

Samples were prepared using an automated vitrification robot (FEI VitrobotTM freeze plunger). The vitrification procedure has been described in details elsewhere [29]. Cryo-TEM pictures were obtained with the TEM microscope (TEM JEM 1400 operating at 120kV). Experiments were performed at Solvay Research & Innovation Centre (Aubervilliers, France).

2.2.2. Dynamic Light Scattering (DLS)

DLS measurements were performed with a DLS setup (Vasco-flex, Cordouan Technologies) with a 658 nm laser wavelength at a scattering angle of 90°. The measured autocorrelation function of the intensity $G_2(Q,t)$ can be expressed using the Siegert relation as:

$$G_2(Q,t) = \alpha + \beta g_1^2(Q,t) \quad (1)$$

where Q is the scattering vector, t the time, $g_1(Q,t)$ the normalized field autocorrelation function, α the baseline and β the coherence factor. In the case of a polydisperse system, $g_1(Q,t)$ can be written as:

$$g_1(Q,t) = \sum_i A_i \mathrm{e}^{-D_i Q^2 t} \quad (2)$$

where A_i is the scattered intensity contribution of particles i and D_i their diffusion coefficient. All D_i were calculated using inversion Pade-Laplace algorithm. Considering isolated Brownian spheres, their hydrodynamic radii R_i were calculated from their respective diffusion coefficient using the Stokes-Einstein equation. A detailed description of the technique can be found in the literature [30].

2.2.3. Quartz crystal microbalance with dissipation monitoring (QCM-D)

QCM-D (flow model E1, Q-sense) measures temporal resonance frequency ($\Delta f_n(t)/n$) and dissipation ($\Delta D_n(t)/n$) shifts of a quartz crystal sensor (with a fundamental resonance frequency f_0 of 5 MHz) at different overtone numbers, n. The surface of the quartz that we used was coated with a 50 nm silicon dioxide layer (Qsense, QSX 303). If the adsorbed layer is rigid, thin and uniformly distributed over the quartz surface, frequency shifts are directly proportional to the adsorbed mass according to the Sauerbrey relation [31]. In this case, frequency shifts ($\Delta f_n/n$) are not dependent on the overtone number and the corresponding energy dissipations are low ($\Delta D_n/n < 2\text{x}10^{-6}$). Furthermore, energy dissipation can give information on some particular characteristics of the adsorbed layer: its softness [32–34], its heterogeneity [35], the degree and geometry of its attachment to the surface [36], the existence of hydrodynamic contribution (related to roughness [36,37]) and/or its viscoelastic properties [38–40]. In the latter cases, both frequency ($\Delta f_n(t)/n$) and dissipation ($\Delta D_n(t)/n$) variations are overtone dependent. In our experiments, due to negligible variations in density and viscosity with the addition of surfactants to the solution (see Table 2), we assumed to

have only slight bulk effect contributions on the measured frequency and dissipation shifts [41,42].

Table 2: Measurements at 20°C of the solutions viscosities and densities, with the Low Shear 30 viscometer (from Contraves) and densimeter Anton Paar DMA 4500M, respectively

Investigated solution	AOT concentration [g/L]	SDBS concentration [g/L]	Viscosity [mPa.s]	Density
Brine 15 g/L NaCl	X	X	1.016	1.011
0.6CVC$_M$	0.027	0.005	1.048	1.012
CVC$_M$	0.045	0.009	1.050	1.012
2.4CVC$_M$	0.108	0.021	1.072	1.012

Adsorption measurements were performed at 20°C at a constant flow rate of 0.2 mL/min. First, a baseline was obtained with the brine solution and then the surfactant solution was injected. More details about the technique can be found elsewhere [43–45].

2.2.4. Neutron reflectivity

Specular neutron reflectivity experiments were performed at the Laboratoire Léon Brillouin (LLB) using Time of Flight Reflectometer Hermès. By analogy to the reflection of light, each interface can be defined by a neutron reflective index. In this technique, the reflectivity R, defined as the reflected intensity normalized by the incident intensity, is displayed as a function of the scattering vector Q, normal to the reflecting surface. The shape of the reflectivity profile obtained depends on the composition, the thickness and the roughness of the surfactant layer adsorbed on a silicon wafer with a native silica oxide layer. A more detailed description of the technique can be found in the literature [46].

3. Results and discussion

3.1. Bulk characterization: the structure of the vesicular phase

The Critical Vesicular Concentration of the mixture (called CVC_M) was measured at 1.27×10^{-4} M, equivalent to $0.5CVC_{AOT}$ and $0.44CMC_{SDBS}$ (see Table 1). The fact that CVC_M is lower than the CVC_{AOT} and CMC_{SDBS} means that surfactant aggregates are formed at a lower concentration than if they were alone in brine.

The structure of aggregates formed in the AOT/SDBS mixture was characterized by Cryo-TEM and DLS measurements. Figure 3 shows a Cryo-TEM image of the AOT/SDBS aggregates formed in brine solution. Only a few number of vesicles are visualized because of the very low surfactant concentration analyzed. We observe some spherical unilamellar vesicles, with a diameter varying from 29 nm to 87 nm. Thus, we supposed that the AOT/SDBS mixture solution is mainly composed of unilamellar vesicles. Indeed, if SDBS micelles are in the solution, they cannot be imaged by Cryo-TEM since they are too small.

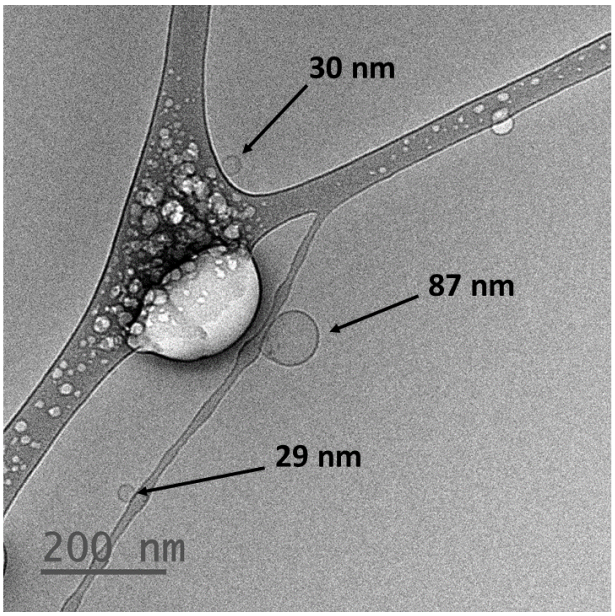

Figure 3 : Cryo-TEM images of AOT (0.099 g/L) / SDBS (0.019 g/L) mixture at 2.2CVC$_M$ in brine solution

Figure 4 displays DLS measurements obtained for the single AOT solution (2.7CVC$_{AOT}$) and the AOT/SDBS mixture (3.6CVC$_M$). We observe that the autocorrelation function (Figure 4a) corresponding to the mixture decays slower than the one of the single AOT solution, indicating the presence of larger aggregates in the mixture solution. The analysis of the vesicular diameters (Figure 4b) shows that the three populations detected for the single AOT solution are also observed in the case of the mixture. However, the average hydrodynamic diameters are significantly larger. We note that the use of the Pade-Laplace analysis is justified by the fact that this algorithm is the most general and does not require any assumptions on the nature of the size distribution of the surfactant aggregates (gaussian, log-normal, etc…) but supposes a discrete number of populations with no distribution. Doing this, we obtained a reliable overview of the global vesicular sizes.

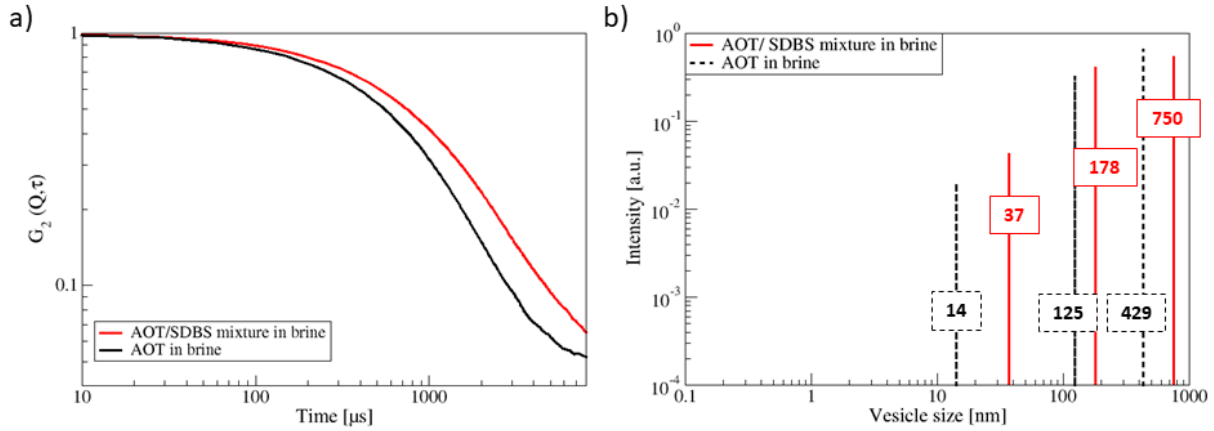

Figure 4 : DLS results comparison between an AOT solution (2.7CVC$_{AOT}$ - black dashes) and an AOT (0.16 g/L) / SDBS (0.032 g/L) mixture solution (3.6CVC$_M$ – red lines) a) Temporal variation of the autocorrelation function b) Distribution of the hydrodynamic diameters

The number distribution presented in Figure 5 shows that the smallest vesicles (37 nm in diameter) prevails in the mixture solution (>99.9%). The main population detected agrees with the two out of three vesicles imaged by Cryo-Tem (see Figure 3: 29 and 30 nm).

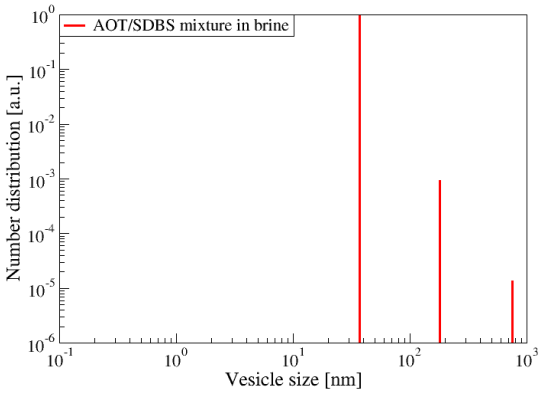

Figure 5 : Number distribution of vesicles in the AOT (0.16 g/L) / SDBS (0.032 g/L) mixture solution ($3.6CVC_M$)

3.2. Adsorption of the AOT/SDBS mixture onto silica at ambient temperature: combination of QCM-D and neutron reflectivity experiments

The adsorption behavior of the AOT/SDBS mixture onto silica was characterized by the combination of QCM-D and neutron reflectivity experiments. Coupling both experimental techniques provides complementary information (investigation of the adsorption kinetics and of the structure of the adsorbed layer at equilibrium) allowing further understanding of the adsorption process of surfactant mixtures in unfavorable conditions.

3.2.1. QCM-D experiments.

Figure 6 gives an overview of the adsorption behavior at equilibrium of the single surfactants (AOT and SDBS) in comparison to their mixture in brine. We consider the equilibrium state to be reached once stabilization in frequency and dissipation shifts (named as plateau values, corresponding to a stable signal for at least 1h).

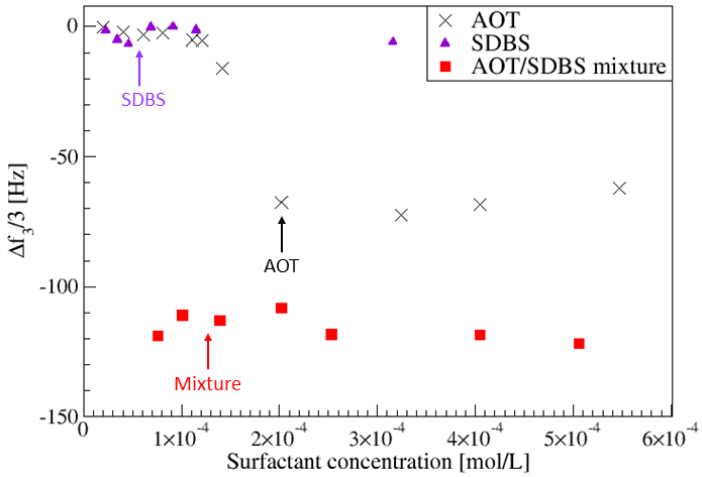

Figure 6: Frequency shifts obtained for the third overtone at the equilibrium state as a function of the molar surfactant concentration of the investigated systems. The arrows show the respective CVC values.

3.2.1.1. Adsorption behavior of the single surfactants below the CAC.

As shown in Figure 6, a slight and similar adsorption has been measured below the CVC_{AOT} and the CMC_{SDBS} ($\Delta f_3/3 < 15$ Hz, as the error bar is estimated to ± 0.5 Hz) and corresponds to monomers' adsorption on the surface.

3.2.1.2. Adsorption behavior of the single surfactants above the CAC.

In Figure 6, we observe that once the respective CVCs are reached, AOT continues to adsorb (demonstrated by the considerable decrease in $\Delta f_3/3$) whereas SDBS does not.

Above the CMC_{SDBS}, SDBS forms micelles in the bulk. The SDBS micelles don't seem to be surface active, thus, the mechanism corresponds to single monomeric adsorption [47,48] and is not modified by the appearance of the surfactant aggregates in the solution.

On the other hand, AOT forms small unilamellar vesicles in solution [26]. Figure 6 clearly shows that vesicles are interacting with the silica surface. The shift in frequency, linked to the important additional mass that is interacting with the surface, i.e vesicular aggregates, is a proof of the change in the adsorption mechanism. The addition of salt to the solution changes the interfacial composition of the surfactant aggregates by decreasing the volume of water trapped in the aggregates. This volume decrease favors closer packing of interfacial headgroups and counterions [49], particularly in vesicular aggregates because of curvature effects, enabling them to interact with the surface because of the decrease of the magnitude of the negative potential near the vesicular surface [50]. It has been previously reported [51] that AOT vesicles adsorb on silica as flattened vesicles.

According to our results, we suggest that the formation of vesicles in solution coupled with the screening of repulsive interactions by salt addition tends to enhance the adsorption of vesicles on silica.

3.2.1.3. Adsorption behaviour of the surfactant mixture.

Considering the surfactant mixture, we observe frequency shifts (≈120 Hz) that are larger than those of single AOT, explained by the presence of larger vesicles in the mixture solution (Figure 4b). Significant frequency shifts were also measured at concentrations where practically no adsorption had been observed with the corresponding single surfactants (Figure 6). Adsorption occurs at lower concentrations in the mixture system as if the mixture of the two surfactants enhanced the adsorption phenomenon. The earlier appearance of vesicular aggregates in the mixture solution (CVC_M being equivalent to $0.5CVC_{AOT}$ and $0.44CMC_{SDBS}$) explains the observed result.

3.2.1.4. Analysis of the QCM-D curves.

Different kinetics are observed as a function of the investigated system (Figure 7). We particularly highlight a sharp increase in the initial adsorption rate for AOT above its CAC (Figure 7b), that can be explained by the faster diffusion to the surface of smaller single AOT vesicles. The adsorption kinetics of the mixture are slower than those of single AOT and depend on the CVC_M. Kinetics are modified by the increase in the total surfactant concentration (between $1.1CVC_M$ and $2.4CVC_M$), which increases the number of vesicles in solution that can interact with the surface. Slow kinetics of the mixture can be explained by the fact that interactions are less favorable than in the case of single AOT. Thus, the time required to reach the equilibrium is longer. This might be due to the fact that mixture vesicles

are composed of both AOT and SDBS, changing the degree of interactions with the silica surface. In the case of 1.1CVC$_M$ kinetics are extremely slow, this is attributed to the very low concentration.

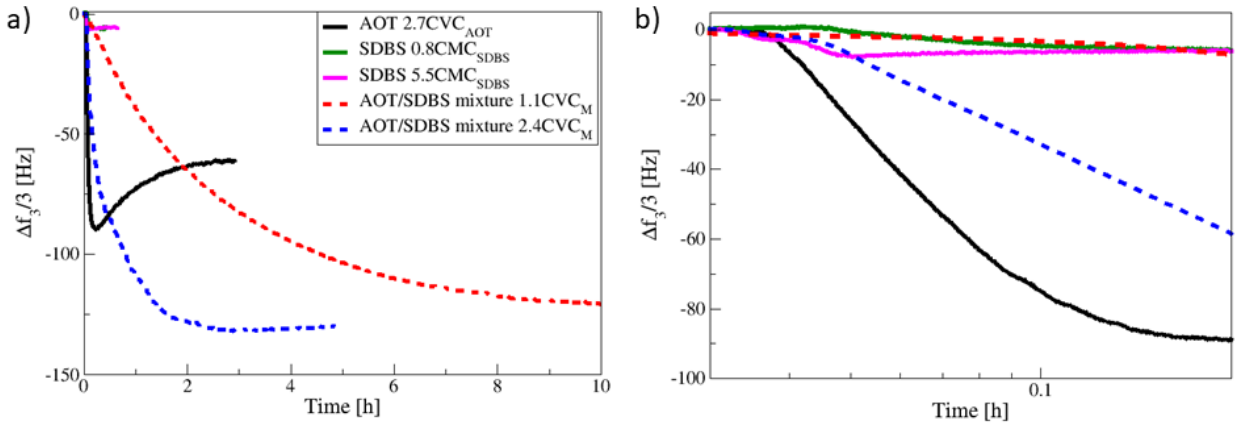

Figure 7 : a) Kinetics measurements obtained with the temporal evolution of the frequency shift for the third overtone during the adsorption of the investigated surfactant systems on silica b) Zoom located at the beginning step of the adsorption process

Figure 8 shows frequency and dissipation shifts (for n=3) as a function of time for the single AOT and the AOT/SDBS mixture above their respective CACs. The curves shape of the mixture is similar to those observed in the literature [60] when intact vesicles adsorb to the surface (monotonically growing signal). However, for single AOT, a rearrangement step is highlighted corresponding to a decrease in the absolute values of frequency and dissipation shifts. One explanation is the flattening of AOT vesicles on the surface [61] as reported elsewhere [51]. Indeed, Van der Veen et al. [56] have shown that the structural stability and flexibility of protein aggregates influence the adsorption process, particularly under electrostatically repulsive conditions. The deformation is possible for a vesicle because of their rather soft and flexible structure [57]. Above the CVC$_M$, we assume the adsorption of intact vesicles as we do not observe any restructuration of the adsorbed layer.

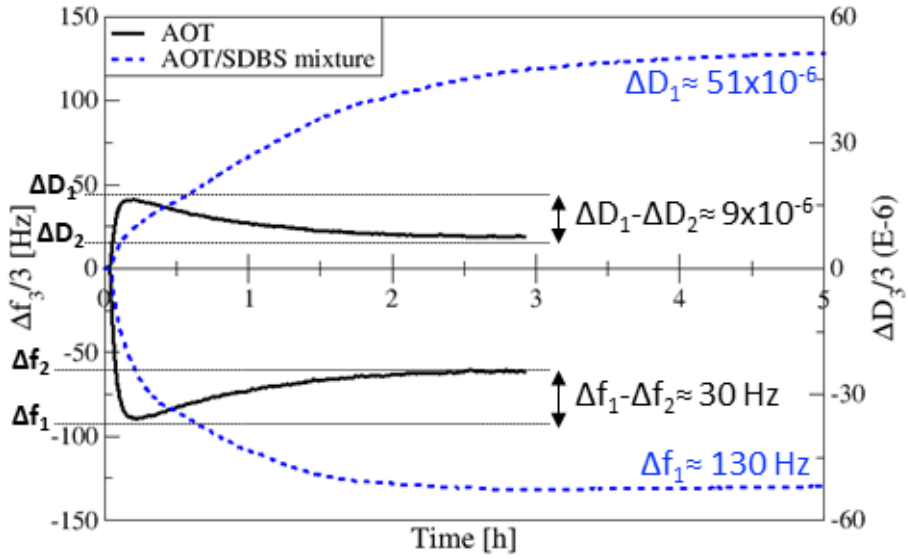

Figure 8 : Kinetics curves for the third overtone number obtained for the single AOT at 2.7CVC$_{AOT}$ (black lines) and the AOT/SDBS mixture at 2.4CVC$_{M}$ (dashed blue lines)

Figure 9 and Figure 10 display results obtained with the mixture for surfactant concentrations below and above, the critical aggregation concentration (CVC$_{AOT}$ or CMC$_{SDBS}$) of the single surfactants in brine. Given the very large dissipations, the QCM-D signal is very overtone dependent and related to the presence of a soft adsorbed layer probably composed of intact vesicles as we do not observe any restructuration step. Possible explanations of the large responses observed could be the adsorption of a heterogeneous layer and/or a weak attachment of vesicles to the surface [36]. We note an increase in the frequency shifts at long times for concentrations above 2.0CVC$_{M}$, which correspond to an AOT concentration above the 1.0CVC$_{AOT}$ of the single component. This increase can be attributed to a slight increase in the solution viscosity due to the appearance of single AOT vesicles in the solution that probably coexist with mixed AOT/SDBS vesicles.

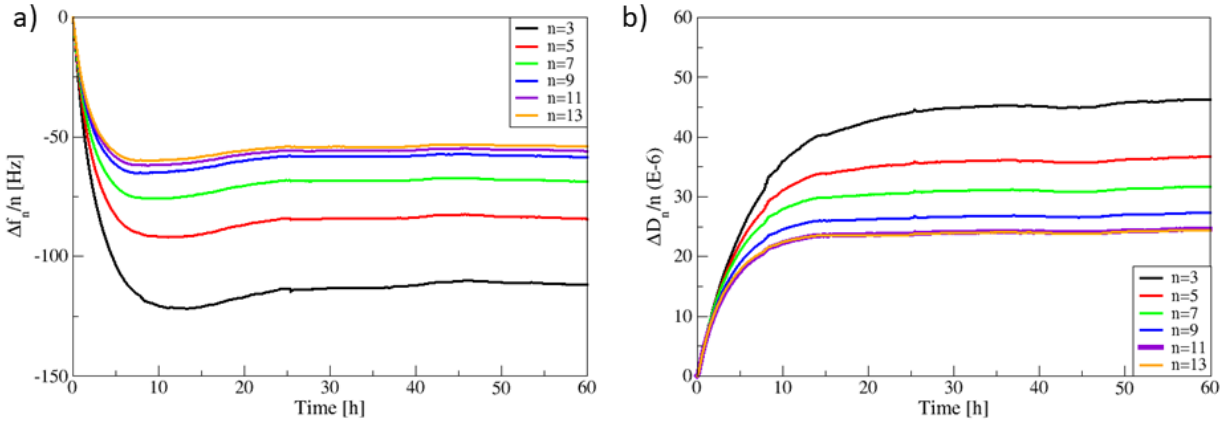

Figure 9: QCM-D plots: a) Frequency shifts and b) Dissipation shifts versus time obtained at different overtones for the adsorption of an AOT (0.55CVC$_{AOT}$=0.05 g/L) / SDBS (0.5CMC$_{SDBS}$=0.01 g/L) mixture at 1.1CVC$_{M}$ in brine on silica

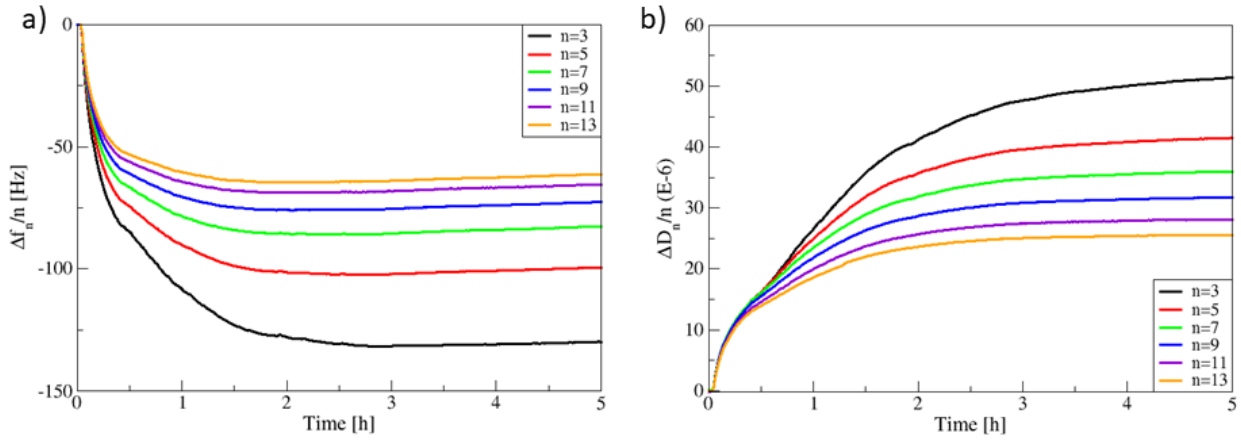

Figure 10: QCM-D plots: a) Frequency shifts and b) Dissipation shifts versus time obtained at different overtones for the adsorption of an AOT (1.2CVC_{AOT}=0.11 g/L) / SDBS (1.06CMC_{SDBS}=0.021 g/L) mixture at 2.4CVC_M in brine on silica

3.2.2. Neutron reflectivity experiments.

The adsorption of the mixture above the CVC_M was also measured by neutron reflectivity experiments. Figure 11 presents the reflectivity profiles of the brine, the single AOT (2.7CVC_{AOT}) and of the AOT/SDBS mixture (2.2CVC_M) on silica. For both solutions containing surfactants an oscillation in the reflectivity profile can be observed, whereas the brine signal is flat (Figure 11b). Data representation in the RQ^4 vs Q form enables to highlight the effect of surfactants as it is known that reflectivity decays at large Q values as Q^{-4} for systems with sharp bare interfaces. We note that the observed oscillation in the mixture profile, providing an evidence of the presence of an adsorbed layer, is less pronounced than the one obtained with the single AOT.

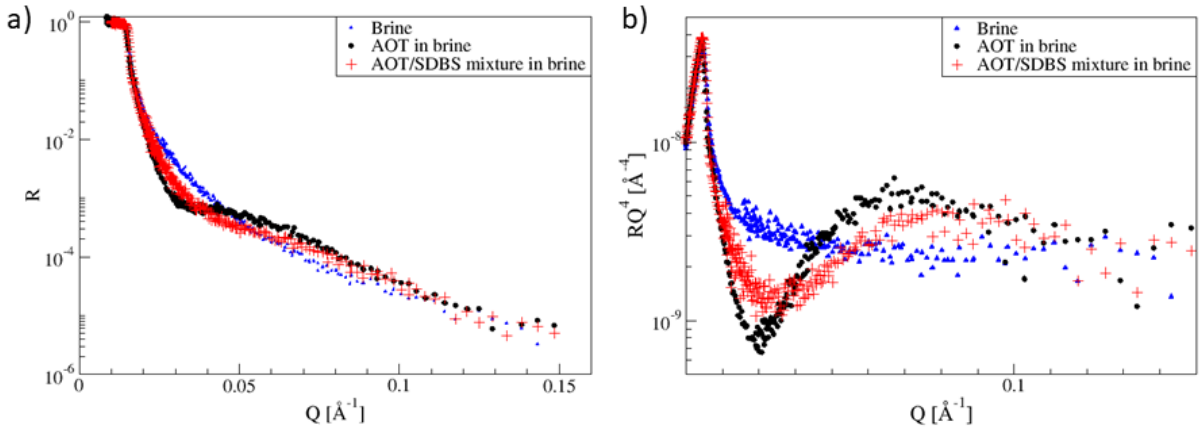

Figure 11 : Neutron reflectivity profiles obtained in D_2O brine a) Comparison between data obtained for the bare silica surface in D_2O brine (blue triangle), the single AOT (0.24 g/L) at 2.7CVC_{AOT} (black circle) and the AOT (0.099 g/L)/SDBS (0.02 g/L) mixture at 2.2CVC_M (red plus). It can be noted that even if the AOT concentration studied was not the same, the comparison remained valid since the adsorbed layer formed with the single AOT is completed at the CVC_{AOT}. b) RQ^4 representation for ease of data viewing

In a previous study [51], we have shown that AOT adsorbs as flattened vesicles above the CVC_{AOT}. Thus, by comparing the mixture reflectivity profile with the reflectivity profile obtained in the case of the single AOT, the following assumptions can be made.

First, in both cases, the total reflection (R=1) is observed up to the same critical wave vector Q, itself almost identical to that of a bare silicon wafer in brine. As this critical wave vector Q is a function of the mean adsorbed layer scattering length density and thus of the chemical composition of the profile, we suppose the adsorbed layer being highly hydrated.

Then, we observe that the oscillation amplitude of the reflectivity profile of the mixture is smaller than the amplitude of the single AOT. The magnitude of the amplitude is related to contrast variation, thus to the different scattering potentials between the components of the surface, the adsorbed layer and finally the bulk. The more pronounced difference in scattering length densities (SLD) will give the more pronounced amplitude. Therefore, we can deduce from the reflectivity profile of the mixture that the adsorbed layer is more hydrated than that of the single AOT as it is composed of a higher number of water molecules (inside the vesicles) which makes the SLD of the adsorbed layer closer to the one of the bulk, while the SLD of the single AOT layer is closer to the SLD of a 100% AOT layer, rendering the contrast with the bulk more important.

Finally, the fact that the oscillation period is slightly widened for the mixture indicates that its adsorbed layer is thinner than the AOT layer. QCM-D indicates no rearrangement step thus no vesicles flattening. Thus the “thinner” adsorbed layer, as the mixed vesicles are larger than the single ones, can be explained by the “heterogeneity” argument, and the probable scattered layer is highlighted in Figure 12.

Summarizing, the adsorbed layer of the mixture seems to be thinner and containing more water molecules than that of the single AOT. This observation is surprising as we have demonstrated by DLS measurements (Figure 4) that AOT/SDBS vesicles are larger (37 nm diameter) than the single AOT vesicles (14 nm diameter). A possible explanation might be that the adsorbed layer is highly heterogeneous and composed of vesicles of different diameters (probably mixed vesicles and single AOT vesicles). We suppose that only the layer close to the silica surface, considering the smallest vesicles, could be detected by the measurement, as a minimum surfactant concentration (contrast with the bulk) is necessary (Figure 12). In fact, the outer part of the larger vesicles might be difficultly visualized as they include a substantial water volume. Thus, neutron reflectivity does not allow the entire characterization of the adsorbed layer of the mixture, however it proves that adsorption takes place. We note that the probable non-negligible silica surface heterogeneity could explain the adsorption of mixture vesicles.

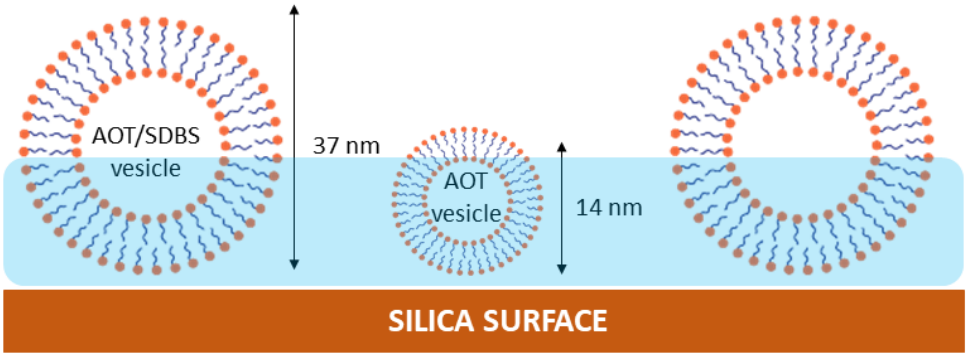

Figure 12: Scheme of the proposed assumption of the mixture adsorbed layer. The part highlighted in blue corresponds to the part probably only visible with this technique because of sufficient contrast

4. Conclusion

In this study, we focused on the adsorption behavior of a mixture of two anionic surfactants (AOT and SDBS) and compared it to the adsorption behavior of single AOT and SDBS in brine solution.

In a first step, we characterized aggregates formed in the bulk solution by means of Cryo-TEM and DLS. Whereas surfactant aggregates in the form of vesicles for AOT and micelles for SDBS above their critical aggregation concentration are obtained, the combination of both gives rise to the formation of aggregates at concentrations even below the CVC_{AOT} and CMC_{SDBS}. Cryo-TEM images provided evidence of the formation of unilamellar vesicles. Based on DLS measurements we could show that mixture vesicles are larger than those of single AOT.

In order to provide further comprehension of the adsorption of surfactant mixtures, we combined QCM-D and neutron reflectivity measurements. They provide complementary information on the adsorption process, its kinetics and the possible final structure of the adsorbed layer. Both techniques confirmed that the mixture adsorbs to the silica surface. We showed that at identical ionic strength conditions, above the respective CVC, AOT adsorbs on silica as a layer composed of packed flattened vesicles, SDBS does not adsorb and the mixture adsorbs as an inhomogeneous layer composed of intact vesicles of different sizes. Mixture adsorption occurs at concentrations where no adsorption is observed with the individual surfactants. This suggests that the structure of the aggregates formed in the bulk has a non-negligible impact on the adsorption phenomenon. Indeed, the presence of vesicles seems to enhance the adsorption in the case of the mixture. We also showed with the dissipation's measurements (QCM-D) that the adsorbed layer of the mixture is more heterogeneous and weakly attached to the surface. This might be attributed to the interactions that may be more unfavorable than in the case of the single AOT system. Finally, we stated that the adsorption kinetics of the mixture are slower particularly in the case of very low concentrations. For both AOT and the surfactant mixture, the addition of a substantial amount of salt enhances the adsorption on silica.

Author statement and acknowledgements

All authors contribute equally to this work.

The authors thank A. Vacher (Solvay, Aubervilliers) and M. Airiau (Solvay, Aubervilliers) for their contributions in Cryo-TEM measurements; J. Jestin (LLB) and H. Perrot (Sorbonne University) for many useful discussions on neutron reflectivity and QCM-D experiments respectively. We also acknowledge the Laboratoire Léon Brillouin for beam time allocation.

References

[1] J. Thavorn, J.J. Hamon, B. Kitiyanan, A. Striolo, B.P. Grady, Competitive surfactant adsorption of AOT and tween 20 on gold measured using a quartz crystal microbalance with dissipation, Langmuir. 30 (2014) 11031–11039. https://doi.org/10.1021/la502513p.

[2] C. Gutig, B.P. Grady, A. Striolo, Experimental studies on the adsorption of two surfactants on solid-aqueous interfaces: Adsorption isotherms and kinetics, Langmuir. 24 (2008) 13814. https://doi.org/10.1021/la8032034.

[3] M.S. Hellsing, A.R. Rennie, A. V. Hughes, Effect of concentration and addition of ions on the adsorption of aerosol-OT to sapphire, Langmuir. 26 (2010) 14567–14573. https://doi.org/10.1021/la101969p.

[4] R. Bordes, J. Tropsch, K. Holmberg, Adsorption of dianionic surfactants based on amino acids at different surfaces studied by QCM-D and SPR, Langmuir. 26 (2010) 10935–10942. https://doi.org/10.1021/la100909x.

[5] J.J.R. Stålgren, J. Eriksson, K. Boschkova, A comparative study of surfactant adsorption on model surfaces using the quartz crystal microbalance and the ellipsometer, J. Colloid Interface Sci. 253 (2002) 190–195. https://doi.org/10.1006/jcis.2002.8482.

[6] I.N. Stocker, K.L. Miller, R.J.L. Welbourn, S.M. Clarke, I.R. Collins, C. Kinane, P. Gutfreund, Adsorption of Aerosol-OT at the calcite/water interface - Comparison of the sodium and calcium salts, J. Colloid Interface Sci. 418 (2014) 140–146. https://doi.org/10.1016/j.jcis.2013.11.046.

[7] P. Somasundaran, L. Zhang, Adsorption of surfactants on minerals for wettability control in improved oil recovery processes, J. Pet. Sci. Eng. 52 (2006) 198–212. https://doi.org/10.1016/j.petrol.2006.03.022.

[8] P. Somasundaran, L. Huang, Adsorption/aggregation of surfactants and their mixtures at solid-liquid interfaces, Adv. Colloid Interface Sci. 88 (2000) 179–208. https://doi.org/10.1016/S0001-8686(00)00044-0.

[9] S. Manne, H.E. Gaub, Molecular Organization of Surfactants at Solid-Liquid Interfaces, Science (80-.). 270 (1995) 1480 LP – 1482. https://doi.org/10.1126/science.270.5241.1480.

[10] X. Wang, S.Y. Lee, K. Miller, R. Welbourn, I. Stocker, S. Clarke, M. Casford, P. Gutfreund, M.W.A. Skoda, Cation bridging studied by specular neutron reflection, Langmuir. 29 (2013) 5520–5527. https://doi.org/10.1021/la400767u.

[11] Z. Huang, Z. Yan, T. Gu, Mixed adsorption of cationic and anionic surfactants from aqueous solution on silica gel, Colloids and Surfaces. 36 (1989) 353–358. https://doi.org/10.1016/0166-6622(89)80249-5.

[12] R. Zhang, P. Somasundaran, Advances in adsorption of surfactants and their mixtures at solid/solution interfaces, Adv. Colloid Interface Sci. 123–126 (2006) 213–229. https://doi.org/10.1016/j.cis.2006.07.004.

[13] P. Somasundaran, E.D. Snell, E. Fu, Q. Xu, Effect of adsorption of non-ionic surfactant and non-ionic-anionic surfactant mixtures on silica-liquid interfacial properties, Colloids and Surfaces. 63 (1992) 49–54. https://doi.org/10.1016/0166-6622(92)80068-D.

[14] M. Muherei, R. Junin, Equilibrium Adsorption Isotherms of Anionic, Nonionic Surfactants and Their Mixtures to Shale and Sandstone, Mod. Appl. Sci. 3 (2009). https://doi.org/10.5539/mas.v3n2p158.

[15] J.J. Lopata, J.H. Harwell, J.F. Scamehorn, Adsorption of Binary Anionic Surfactant Mixtures on α-Alumina, in: Surfactant-Based Mobil. Control, American Chemical Society, 1988: pp. 10–205. https://doi.org/doi:10.1021/bk-1988-0373.ch010.

[16] S. Vora, A. George, H. Desai, P. Bahadur, Mixed micelles of some anionic-anionic, cationic-cationic, and ionic-nonionic surfactants in aqueous media, J. Surfactants Deterg. 2 (1999) 213–221. https://doi.org/10.1007/s11743-999-0076-5.

[17] K. Shinoda, The critical micelle concentration of soap mixtures (two-component mixture), J. Phys. Chem. 58 (1954) 541–544. https://doi.org/10.1021/j150517a007.

[18] P.M. Holland, D.N. Rubingh, Mixed Surfactant Systems, in: Mix. Surfactant Syst., American Chemical Society, 1992: pp. 1–2. https://doi.org/doi:10.1021/bk-1992-0501.ch001.

[19] Y. Muto, K. Esumi, K. Meguro, R. Zana, Aggregation behavior of mixed fluorocarbon and hydrocarbon surfactants in aqueous solutions, J. Colloid Interface Sci. 120 (1987) 162–171. https://doi.org/10.1016/0021-9797(87)90335-3.

[20] S.J. Burkitt, R.H. Ottewill, J.B. Hayter, B.T. Ingram, Small angle neutron scattering studies on micellar systems part 1. Ammonium octanoate, ammonium decanoate and ammonium perfluoroocatanoate, Colloid Polym. Sci. 265 (1987) 619–627. https://doi.org/10.1007/BF01412778.

[21] K. Esumi, Y. Sakamoto, K. Yoshikawa, K. Meguro, Properties of mixed bilayers of hydrocarbon and fluorocarbon surfactants on monodispersed ferric hydro sols, Colloids and Surfaces. 36 (1989) 1–11. https://doi.org/10.1016/0166-6622(89)80090-3.

[22] K. Iler, The Chemistry of Silica Solubility, Polymerization, Colloid and Surface Properties and Biochemistry of Silica, John Wiley Sons Inc. (1979).

[23] O.G. Singh, K. Ismail, Micellization behavior of mixtures of sodium dioctylsulfosuccinate with sodium dodecylsulfate in water, J. Surfactants Deterg. 11 (2008) 89–96. https://doi.org/10.1007/s11743-007-1058-y.

[24] N.R. Tummala, L. Shi, A. Striolo, Molecular dynamics simulations of surfactants at the silica-water interface: Anionic vs nonionic headgroups, J. Colloid Interface Sci. 362 (2011) 135–143. https://doi.org/10.1016/j.jcis.2011.06.033.

[25] Z.X. Li, J.R. Lu, R.K. Thomas, Neutron reflectivity studies of the adsorption of aerosol-OT at the air/water interface: The surface excess, Langmuir. 13 (1997) 3681–3685. https://doi.org/10.1021/la9608472.

[26] J. Wolanin, L. Barre, C. Dalmazzone, D. Bauer, A complete characterization of the structure of the vesicular phase in AOT — Brine system in the diluted region of the phase diagram, Colloids Surfaces A Physicochem. Eng. Asp. 559 (2018). https://doi.org/10.1016/j.colsurfa.2018.09.052.

[27] D.C.H. Cheng, E. Gulari, Micellization and intermicellar interactions in aqueous sodium dodecyl benzene sulfonate solutions, J. Colloid Interface Sci. 90 (1982) 410–423. https://doi.org/10.1016/0021-9797(82)90308-3.

[28] L. Zhai, M. Zhao, D. Sun, J. Hao, L. Zhang, Salt-induced vesicle formation from single anionic surfactant SDBS and its mixture with LSB in aqueous solution, J. Phys. Chem. B. 109 (2005) 5627–5630. https://doi.org/10.1021/jp044596e.

[29] J. Kuntsche, J.C. Horst, H. Bunjes, Cryogenic transmission electron microscopy (cryo-TEM) for studying the morphology of colloidal drug delivery systems, Int. J. Pharm. 417 (2011) 120–137. https://doi.org/10.1016/j.ijpharm.2011.02.001.

[30] D.K. Carpenter, Dynamic Light Scattering with Applications to Chemistry, Biology, and Physics (Berne, Bruce J.; Pecora, Robert), J. Chem. Educ. 54 (1977) A430. https://doi.org/10.1021/ed054pA430.1.

[31] G. Sauerbrey, Verwendung von Schwingquarzen zur Wägung dünner Schichten und zur Mikrowägung, Zeitschrift Für Phys. 155 (1959) 206–222. https://doi.org/10.1007/BF01337937.

[32] N.J. Cho, C.W. Frank, B. Kasemo, F. Höök, Quartz crystal microbalance with dissipation monitoring of supported lipid bilayers on various substrates, Nat. Protoc. 5 (2010) 1096–1106. https://doi.org/10.1038/nprot.2010.65.

[33] M.C. Dixon, Quartz crystal microbalance with dissipation monitoring: Enabling real-time characterization of biological materials and their interactions, J. Biomol. Tech. 19 (2008) 151–158.

[34] F. Höök, M. Rodahl, P. Brzezinski, B. Kasemo, Energy dissipation kinetics for protein and antibody-antigen adsorption under shear oscillation on a quartz crystal microbalance, Langmuir. 14 (1998) 729–734. https://doi.org/10.1021/la970815u.

[35] D. Johannsmann, I. Reviakine, E. Rojas, M. Gallego, Effect of sample heterogeneity on the interpretation of QCM(-D) data: Comparison of combined quartz crystal microbalance/atomic force microscopy measurements with finite element method modeling, Anal. Chem. 80 (2008) 8891–8899. https://doi.org/10.1021/ac8013115.

[36] D. Johannsmann, I. Reviakine, R.P. Richter, Dissipation in films of adsorbed nanospheres studied by quartz crystal microbalance (QCM), Anal. Chem. 81 (2009)

8167–8176. https://doi.org/10.1021/ac901381z.

[37] K. Rechendorff, M.B. Hovgaard, M. Foss, F. Besenbacher, Influence of surface roughness on quartz crystal microbalance measurements in liquids, J. Appl. Phys. 101 (2007) 114502. https://doi.org/10.1063/1.2735399.

[38] S.X. Liu, J.T. Kim, Application of Kevin—Voigt Model in Quantifying Whey Protein Adsorption on Polyethersulfone Using QCM-D, J. Lab. Autom. 14 (2009) 213–220. https://doi.org/10.1016/j.jala.2009.01.003.

[39] F. Höök, B. Kasemo, T. Nylander, C. Fant, K. Sott, H. Elwing, Variations in coupled water, viscoelastic properties, and film thickness of a Mefp-1 protein film during adsorption and cross-linking: A quartz crystal microbalance with dissipation monitoring, ellipsometry, and surface plasmon resonance study, Anal. Chem. 73 (2001) 5796–5804. https://doi.org/10.1021/ac0106501.

[40] M. V Voinova, M. Rodahl, M. Jonson, B. Kasemo, Viscoelastic Acoustic Response of Layered Polymer Films at Fluid-Solid Interfaces: Continuum Mechanics Approach, Phys. Scr. 59 (1999) 391–396. https://doi.org/10.1238/physica.regular.059a00391.

[41] K.K. Kanazawa, J.G. Gordon, Frequency of a Quartz Microbalance in Contact with Liquid, Anal. Chem. 57 (1985) 1770–1771. https://doi.org/10.1021/ac00285a062.

[42] K. Keiji Kanazawa, J.G. Gordon, The oscillation frequency of a quartz resonator in contact with liquid, Anal. Chim. Acta. 175 (1985) 99–105. https://doi.org/10.1016/S0003-2670(00)82721-X.

[43] D. Johannsmann, The quartz crystal microbalance in soft matter research: fundamentals and modeling, Springer, 2014. https://doi.org/10.1007/978-3-319-07836-6.

[44] M. Rodahl, F. Höök, B. Kasemo, QCM Operation in Liquids: An Explanation of Measured Variations in Frequency and Q Factor with Liquid Conductivity, Anal. Chem. 68 (1996) 2219–2227. https://doi.org/10.1021/ac951203m.

[45] M. Rodahl, F. Höök, A. Krozer, P. Brzezinski, B. Kasemo, Quartz crystal microbalance setup for frequency and Q-factor measurements in gaseous and liquid environments, Rev. Sci. Instrum. 66 (1995) 3924–3930. https://doi.org/10.1063/1.1145396.

[46] J. Penfold, R.K. Thomas, The application of the specular reflection of neutrons to the study of surfaces and interfaces, J. Phys. Condens. Matter. 2 (1990) 1369–1412. https://doi.org/10.1088/0953-8984/2/6/001.

[47] J.J. Hamon, R.F. Tabor, A. Striolo, B.P. Grady, Atomic Force Microscopy Force Mapping Analysis of an Adsorbed Surfactant above and below the Critical Micelle Concentration, Langmuir. 34 (2018) 7223–7239. https://doi.org/10.1021/acs.langmuir.8b00574.

[48] A. Striolo, B.P. Grady, Surfactant Assemblies on Selected Nanostructured Surfaces: Evidence, Driving Forces, and Applications, Langmuir. 33 (2017) 8099–8113. https://doi.org/10.1021/acs.langmuir.7b00756.

[49] C. Liu, Y. Wang, Y. Gao, Y. Zhang, L. Zhao, B. Xu, L.S. Romsted, Effects of

interfacial specific cations and water molarities on AOT micelle-to-vesicle transitions by chemical trapping: The specific ion-pair/hydration model, Phys. Chem. Chem. Phys. 21 (2019) 8633–8644. https://doi.org/10.1039/c8cp05987j.

[50] S. Nir, C. Newton, D. Papahadjopoulos, Binding of Cations to Phosphatidylserine Vesicles, Bioelectrochemistry Bioenerg. 5 (1978) 116–133. https://doi.org/10.1016/0302-4598(87)87012-5.

[51] J. Wolanin, L. Barré, C. Dalmazzone, D. Frot, J. Jestin, H. Perrot, D. Bauer, Insight into Kinetics and Mechanisms of AOT Vesicle Adsorption on Silica in Unfavorable Conditions, Langmuir. 36 (2020) 1937–1949. https://doi.org/10.1021/acs.langmuir.9b03897.

[52] J.S. Puskin, Divalent cation binding to phospholipids: An EPR study, J. Membr. Biol. 35 (1977) 39–55. https://doi.org/10.1007/BF01869939.

[53] F.J. Allen, C.L. Truscott, P. Gutfreund, R.J.L. Welbourn, S.M. Clarke, Potassium, Calcium, and Magnesium Bridging of AOT to Mica at Constant Ionic Strength, Langmuir. 35 (2019) 5753–5761. https://doi.org/10.1021/acs.langmuir.9b00533.

[54] F.J. Allen, L.R. Griffin, R.M. Alloway, P. Gutfreund, S.Y. Lee, C.L. Truscott, R.J.L. Welbourn, M.H. Wood, S.M. Clarke, An Anionic Surfactant on an Anionic Substrate: Monovalent Cation Binding, Langmuir. 33 (2017) 7881–7888. https://doi.org/10.1021/acs.langmuir.7b01837.

[55] A.W. Cross, G.G. Jayson, The Effect of Small Quantities of Calcium on the Adsorption of Sodium Dodecyl Sulfate and Calcium at the Gas-Liquid Interface, J. Colloid Interface Sci. 162 (1994) 45–51. https://doi.org/https://doi.org/10.1006/jcis.1994.1006.

[56] M. Van Der Veen, W. Norde, M.C. Stuart, Electrostatic interactions in protein adsorption probed by comparing lysozyme and succinylated lysozyme, Colloids Surfaces B Biointerfaces. 35 (2004) 33–40. https://doi.org/10.1016/j.colsurfb.2004.02.005.

[57] K. Dimitrievski, B. Kasemo, Influence of lipid vesicle composition and surface charge density on vesicle adsorption events: A kinetic phase diagram, Langmuir. 25 (2009) 8865–8869. https://doi.org/10.1021/la9025409.

[58] J. Meissner, A. Prause, B. Bharti, G.H. Findenegg, Characterization of protein adsorption onto silica nanoparticles: influence of pH and ionic strength, Colloid Polym. Sci. 293 (2015) 3381–3391. https://doi.org/10.1007/s00396-015-3754-x.

[59] S.B. Velegol, B.D. Fleming, S. Biggs, E.J. Wanless, R.D. Tilton, Counterion effects on hexadecyltrimethylammonium surfactant adsorption and self-assembly on silica, Langmuir. 16 (2000) 2548–2556. https://doi.org/10.1021/la9910935.

[60] G.J. Hardy, R. Nayak, S. Munir Alam, J.G. Shapter, F. Heinrich, S. Zauscher, Biomimetic supported lipid bilayers with high cholesterol content formed by α-helical peptide-induced vesicle fusion, J. Mater. Chem. 22 (2012) 19506–19513. https://doi.org/10.1039/c2jm32016a.

[61] E. Reimhult, F. Höök, B. Kasemo, Vesicle adsorption on SiO2 and TiO2: Dependence

on vesicle size, J. Chem. Phys. 117 (2002) 7401–7404.
https://doi.org/10.1063/1.1515320.